Wood Science and Technology (2025) 59:10
https://doi.org/10.1007/s00226-024-01616-4

ORIGINAL

Early detection of heartwood rot caused by *Fistulina hepatica* in *Castanea sativa* productive coppices through low-invasive resistance drilling

Andreu Meijer[1,2] · E. Jordán Muñoz-Adalia[2,3] · Eduard Correal-Mòdol[2] · Carlos Colinas[1,2]

Received: 24 May 2024 / Accepted: 25 September 2024 / Published online: 13 November 2024
© The Author(s) 2024

Abstract

Chestnut Red Stain (CRS) is a heartwood discoloration that widely affects *Castanea sativa* Mill. productive coppice stands in the northeast of Spain. At the early stages of infection, the structural properties of the wood are not affected, but still its economic value drops up to 70% due to the rejection of this wood. This disease is caused by the fungus *Fistulina hepatica* (Schaeff.) With. and causes uncertainty to forest managers since the fungal infection is virtually impossible to detect before felling. The objective of this work was to develop an efficient detection method to evaluate the presence of *F. hepatica* in early stages of productive periods. A total of 72 chestnuts were analyzed through molecular methods to determine the presence of *F. hepatica* and with an IML resistance drill to characterize their wood. Thirteen wood quality indices were calculated and their correlation with the presence of the pathogen was evaluated using linear mixed models. We found clear differences between healthy and infected trees in four indices. A new specific index (Chestnut Red Stain Danger index) was designed to estimate the probability of infection by *F. hepatica*. The results support the hypothesis that the early presence of *F. hepatica* is detectable through inexpensive and fast mechanical methods early in a rotation. The results of this work will help forest managers evaluate the incidence of CRS, as well as it establishes a novel methodology for further development of resistance drilling techniques for heartwood rot detection.

✉ Andreu Meijer
amm34@alumnes.udl.cat

[1] Department of Forestry and Agricultural Science and Engineering, University of Lleida, Av. de l'Alcalde Rovira Roure 191, 25198 Lleida, Spain

[2] Forest Science and Technology Centre of Catalonia (CTFC), Carretera St. Llorenç de Morunys, km.2 Solsona, 25280 Catalonia, Spain

[3] Department of Agroforestry Sciences, iuFOR University of Valladolid, ETSIAA Palencia; Av. Madrid, 57, 34071 Palencia, Spain

Introduction

Sweet chestnut (*Castanea sativa* Mill.; Fagaceae) is a multipurpose forestry species with a wide distribution across Europe that has been cultivated for fruit and timber for centuries (Buonincontri et al. 2015; Conedera et al. 2004; Krebs et al. 2022). Chestnut produces high-quality timber, rich in tannins, that confer high resistance to rot fungi (Thaler et al. 2014) and make it particularly suitable for outdoor use (Conedera et al. 2016; Dogu et al. 2011).

Since the 1980s, *C. sativa* is facing a generalized silvicultural abandonment in the north-east region of Spain, caused by the widespread Chestnut Blight (causal agent *Cryphonectria parasitica* (Murrill) M.E. Barr), uncertain market conditions and, since the 1990s, the irruption of the heartwood discoloration known as Chestnut Red Stain (CRS) [causal agent *Fistulina hepatica* (Schaeff.) With. (Basidiomycota; Fistulinaceae)]. Sweet chestnut larger diameter logs fetch very high prices in the market, but when affected by CRS, timber value can drop by 70% (Yurkewich et al. 2017) posing a major challenge for the chestnut industry (Regué et al. 2019). The fungal infection is virtually impossible to detect until the trees are felled since it does not cause any external symptom, except for occasional appearance of conspicuous red fruiting bodies in the lower part of the trunk, thus adding to the insecurity of forest managers. When the trees become infected, they are logged at early ages, when CRS only affects a small proportion of the central heartwood and are consequently marked as poles. In case of CRS-free coppice stands, their rotation (i.e., age or number of years at which it is planned to harvest a coetaneous stand) could be extended to achieve a much higher economic return for their timber in the market for the highest quality saw logs of large diameter. In consequence, the absence of routinary methods for early detection of the disease, promotes that forest owners abandon chestnut production since uncertainty in market prices makes it economically unattractive (Vericat et al. 2012).

Several techniques have been used to detect the presence of heart rot in mature trees (Ondrejka et al. 2021). In the 1990s a low-destructive technique, resistance drilling, became available to determine the variation of resistance to penetration of wood. The method consists of penetrating the wood with a drill at a constant speed measuring its energy consumption (Rinn et al. 1996). A drilling resistance instrument uses a 3 mm thick drilling needle at a known forward feed speed (cm/min) and the rotation rate (revolutions per minute or rpm) and the instrument records the penetration resistance every 0.1 mm, measuring it by the relative amplitude percentage (Instrumenta Mechanik Labor System GmbH 2023). This technique is commonly used to evaluate the soundness of wooden structural elements as beams and artistic elements in buildings (Acuña et al. 2011; Kappel and Mattheck 2003), although its use is becoming more extended in urban areas for assessing the safety of trees in public spaces (Wang and Allison 2008; Papandrea et al. 2022).

In forestry, this technique is being successfully used to assess the basic density of wood or specific gravity, both highly important properties for productive

species, such as *Eucalyptus* sp. and *Pinus sylvestris* L. (Oliveira et al. 2017; Downes et al. 2018; Fundova et al. 2018). Its use to evaluate the rot incidence in plantation trees has been successfully studied in other species, such as *Abies alba* Mill., *Eucalyptus globulus* Labill. and *Populus* sp. (Johnstone et al. 2010; Tamantini et al. 2022), although it requires a visual inspection of the interior of the trunk/stem after its analysis (Johnstone et al. 2007). In sweet chestnut, Tamantini et al. (2022) reported a resistance decrease to drilling of wood affected by advanced wood discoloration, although the specific causal agent was not described. Consequently, its use to evaluate early developing wood decay in standing trees for wood production is as incipient as promising, nevertheless forest science still lacks validated methods for its use in the detection of a variety of wood borer insects and rot pathogens.

Fistulina hepatica has been reported to not alter the mechanical properties of the infected wood at early stages (Correal-Mòdol 2013; Schwarze et al. 2000a, b). When colonization begins, the hyphae of *F. hepatica* pass between cells mainly through pits, without causing noticeable cell wall degradation, which suggests that it initially consumes mainly phenolic compounds and tannins (Cartwright 1937; Schwarze et al. 2000a) located in the corners of xylematic cells and in the intercellular spaces (Giovando et al. 2019). This mycelial development allows the hyphae to advance throughout the xylem without weakening the cell wall structure. Yet the discoloration caused by the deposition of dark debris of polyphenolic compounds in the infected parenchyma cells (Schwarze et al. 2000b) renders the wood unmarketable for the quality timber industry. Although it is acknowledged that the colonization of *F. hepatica* does not lead to significant changes in the mechanical properties of the wood at early stages, we hypothesized that its presence may induce slight alterations that could be detectable through resistance drilling. Consequently, the aims of this work were (i) to evaluate whether the presence of *F. hepatica* causes noticeable variations of wood resistance to drilling that could be detected in standing trees, (ii) to evaluate the impact of *F. hepatica* infection in chestnut wood through the evaluation of main indices based on resistance drilling data, and (iii) to develop a specific index that could support forestry decisions considering the risk of infection by CRS.

Materials and methods

Experimental design

This study was conducted in 2022 in Montseny Natural Park (41°47′N 2°24′E, Catalonia, north-eastern Spain). Data were gathered from five experimental chestnut coppice stands (blocks) of similar age (18 years) when thinned in 2013. The stands had similar conditions with a slope average of 55.90 ± 12.80 %, an average elevation of 769 ± 110 m.a.s.l. and North and North-East aspect, conditions that are reported to favor the apparition of CRS (Regué et al. 2019). The two furthest stands were separated 14 kilometers. Each stand was divided into 3 experimental plots that received different treatments: (Ta) low thinning, that is, removal of dominated trees [i.e extracted basal area (BA) ranged from 36 to 50 %; extracted number of trees

(diameter {D} > 7.5cm) ranged from 48 to 59 %; final tree density ranged from 891 to 1464 trees/ha]; (Tb) selective mixed thinning, low thinning complemented with a selective thinning removing direct competence around the best trees for high-quality timber (i.e extracted BA ranged from 28 to 58 %; extracted number of trees (D > 7.5cm) ranged from 33 to 65 %; final tree density ranged from 955 to 1241 trees/ha); and (Tc) control, no intervention in order to monitor the natural evolution of the stand (i.e tree density ranged from 1528 to 3820 trees/ha). The plots showed initial BA of 31.4 ± 7.38 m^2/ha (mean ± standard deviation) and quadratic mean diameter (QMD) of 12.7 ± 1.81 cm. After the thinnings, the final BA was 22.2 ± 10.27 m^2/ha and QMD of 13.4 ± 1.86 cm.

The presence of *F. hepatica* in the study plots was confirmed in a previous study through molecular methods (Meijer et al. 2024). The infection ranged from 20 % to 100 % of the analyzed trees in each plot. Briefly, in the year 2021, five trees of different stumps were selected in a radius of 10 m from the center of the plot (that is, 75 trees in total). One wood core (depth extended beyond the center of the stem) was extracted 0.3 m aboveground for each tree. The molecular diagnosis (i.e., DNA extraction, amplification by PCR of a *F. hepatica´*s specific ribosomal marker, and sequencing) was performed according to the method described by Regué et al. (2019).

Resistance drilling was measured in August 2022 on five selected trees per plot (i.e., 72 trees; two trees in plot A7 and one in plot A8 died between the sampling periods of 2021 and 2022 and were excluded from the evaluation). The trees were categorized as infected by *F. hepatica* or free of the disease according to molecular results described above (i.e., 38 were infected and 34 free of *F. hepatica*). Drilling resistance was measured with an IML RESI F300-S (IML, Wiesloch, Germany) at 0.30 m above the ground. The IML resistance drill was set to "hardwood" mode, rotation is given by an accumulator drill (GSR 12V, Bosch, Stuttgart Germany) rpm setting was 400. The diameter of each tree was measured at the same drilling height, and drilling depths exceeded the central part of the trunk (average diameter:16.61 ± 3.49 cm). The friction forces when drilling hardwood regarding penetration depth influences the resistance amplitude (Oliveira et al. 2017). To minimize this effect and to ensure CRS detection in the center of the trunk, drilling depth was slightly greater than the length of the radius and the needle was changed after sampling 15 trees to prevent needle wear from affecting the measurements. Each tree was drilled twice in perpendicular directions (i.e., North-South and East-West) resulting in 10 records per plot.

Data processing

Data of each resistogram (graphical representation of the energy consumption of the drill when penetrating the wood) were exported as a numerical matrix using the F-Tools Pro software V1.6 (Instrumenta Mechanik Labor GmbH, Wiesloch, Germany). Records from the initial 20 mm of each resistogram were trimmed from the data analysis since they included the initial advance of the needle (0 values) and values corresponding to bark tissue (not affected by fungal development in any case).

Table 1 Description of the resistance drilling indices. Units; dA: drilling amplitude. Source: Acuña et al. (2011)

Index name	Description	Units	Formula
Average of energy consumption	Average value of energy consumption per centimeter penetrated (A: penetration dept; x: amplitude values of the resistogram)	dA/cm	$Vmed = \frac{\int_0^A f(x)}{0A}$
Variability	Difference of the standard deviation (σ) and coefficient of variation (CV). Dispersion of the sample, indicating the homogeneity of the material	dA	$\mathrm{Var} = \sigma - \mathrm{CV}$
Average of maximums	Average energy consumption of the latewood (M: Maximum value, n: number of "peaks")	dA	$Mmax = \frac{\sum_{i=1}^{n} M_i}{n}$
Average of minimums	Average energy consumption of the earlywood (m: minimum value, n: number of "valleys")	dA	$Mmin = \frac{\sum_{j=1}^{n} m_j}{n}$
Resistance variation	Amplitude difference between the latewood and the earlywood	dA	$Vden = Mmax - Mmin$
Maximum value	Highest value to detect knots or anomalies of extreme density	dA	$\mathrm{V}max$
Minimum value	Lowest value that may indicate cracks, cavities, or other anomalies	dA	$\mathrm{V}min$
Maximum variation	Index to escalate the difference between the average of maximums respect to the average of energy consumption	dA	$\mathrm{Dmax} = Mmax - Vmed$
Minimum variation	Index, in absolute value, to escalate the difference between the average of minimums with respect to the average of energy consumption	dA	$\mathrm{Dmin} = \lvert Mmin - Vmed \rvert$
Difference of maximums	Difference between the maximum value and the average of maximums	dA	$\Delta max = Vmax - Mmax$
Difference of minimums	Difference between the minimum value and the average of minimums	dA	$\Delta min = Vmin - Mmin$
J Value	Difference between the absolute maximum value and total average as percentage of the total average	%	$J = \frac{Mmax - Vmed}{Vmed} \cdot 100$
H Value	Difference between the absolute minimum value and total average as percentage of the total average	%	$H = \frac{\lvert Mmin - Vmed \rvert}{Vmed} \cdot 100$

Trimmed data were used for computing a total of 13 indices (Table 1) to describe each resistogram (Acuña et al. 2011).

Statistical analysis

All statistical analyses were performed in R programming environment (R Core Team 2023). Generalized linear mixed models (GLMMs) that compared the effect of the presence or absence of *F. hepatica* (F) on the different resistance drilling indices using the "lmer" function in the *lme4* package (Bates et al. 2015) were fitted according to the following structure:

$$Y = \text{explicative effect/s} + \text{random effect/s} + \text{residual}$$

where Y is the response variable (wood indicator), explicative effects were the presence/absence of *F. hepatica* (F) and silvicultural treatment (T: control; low thinning; selective mixed thinning) were included as explicative variables in different combinations. Random effects were considered in different combinations to evaluate whether they retained data variability being therefore able to improve model fitness. More specifically, sampled tree (I), plot (P), plot aspect (O) and tree diameter (D) were considered as random in the different fitted models. Sixteen separate models were used in total to evaluate each index. The Akaike´s Information Criteria (AIC) were used as indicators of model quality (parsimony criteria) using the R package AICcmodavg (Mazerolle 2023), together with the significance of the explanatory variable of interest. The most parsimonious model for each resistance drilling index was compared with the corresponding null model (that only included the presence of *F. hepatica* as fixed factor and tree as random factor) using the χ^2 test. Fitness quality of selected models was confirmed through residual analysis and visualization using DHARMa package (Hartig 2022) and the overall fit with the conditional R^2 conducted using the MuMIn package (Barton 2020) in R.

A total amount of 20 logistic GLMs (Generalized Mixed Models; binomial distribution) were computed in R to obtain a predictive model based on those indices that significantly varied with fungal infection (Table 1). The most explicative model (i.e., Model M2p) was selected as explained above and used for providing an estimated probability of CRS infection easy to use and interpret by foresters.

Results

A preliminary observation of the resistance profiles did not allow for clear discrimination between infected and healthy trees (Fig. 1). However, the statistical analyses showed a general reduction of the value of the indices when *F. hepatica* was colonizing the trunk (Table 2). A total of 208 GLMMs were computed (i.e., 16 per resistance drilling index). In all cases, the value of the index was altered in the presence of the fungus, showing a generalized reduction of the index's values except for Dmin, J-value and H-value. The presence of *F. hepatica* significantly

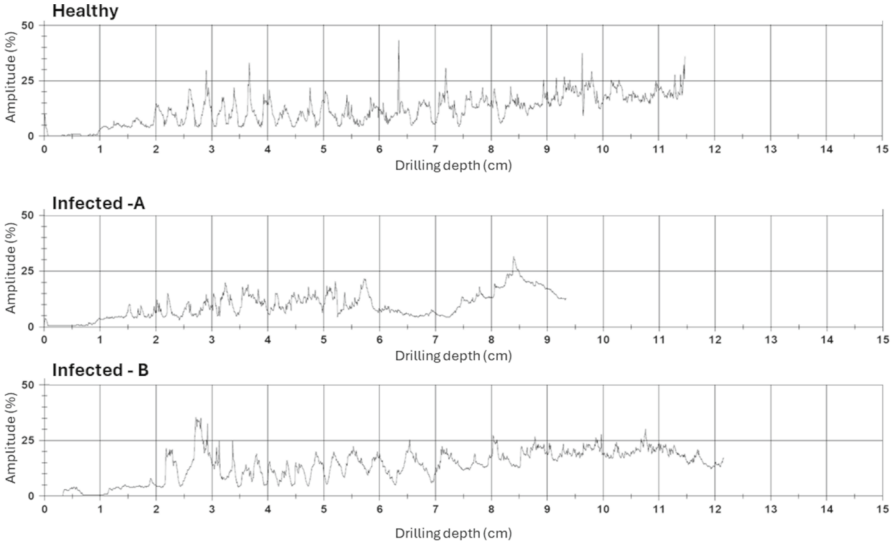

Fig. 1 Resistance drilling profiles of *F. hepatica*-free tree (Healthy, top; ID: C3-52-S; sampling direction north-south; tree diameter: 20 cm) presenting a well-defined annual growth pattern; an infected tree (Infected-A, middle; ID: N3-29-E; sampling direction east-west; tree diameter: 16 cm) presenting a less defined pattern of annual growth together with an evident rot between 6-7.5 cm of drilling depth; and an infected tree (Infected-B, bottom; ID: T4-7-S; sampling direction north-south; tree diameter: 21 cm) presenting a well-defined annual growth without evident signs of rot. All three drilling samples missed the pith

Table 2 Estimated values of analyzed indices in healthy and infected trees

Index[1]	Model[2]	Healthy	Infected	Unit
Vmed	$M0_{Vmed}$	18.42 a	16.51 a	dA/cm
Var	$M0_{Var}$	6.71 a	6.52 a	dA
Mmax	$M0_{Mmax}$	20.37 a	18.19 b	dA
Mmin	$M0_{Mmin}$	17.34 a	15.36 b	dA
Vden	$M0_{Vden}$	3.03 a	2.82 a	dA
Vmax	$M4_{Vmax}$	46.38 a	42.86 a	dA
Vmin	$M0_{Vmin}$	5.04 a	4.17 b	dA
Dmax	$M0_{Dmax}$	1.95 a	1.68 b	dA
Dmin	$M0_{Dmin}$	1.08 a	1.18 a	dA
Δmax	$M4_{\Delta max}$	26.00 a	24.67 a	dA
Δmin	$M0_{\Delta min}$	12.30 a	11.19 a	dA
J	$M4_{J}$	162.66 a	167.54 a	%
H	$M4_{H}$	72.51 a	73.65 a	%

[1]Index abbreviations according to Table 1. [2]Models used for estimating differences between healthy and infected trees according to codes provided in Table 3 and S1. Values followed by the same letter (a-b) are not significantly different at p-value < 0.05. Units; dA: drilling amplitude

affected (p-value < 0.05) the average of maximums (Mmax), average of minimums (Mmin), maximum variation (Dmax) and the minimum value (Vmin) (Table 2).

The silvicultural treatment (T) did not show any significant effect on any of the evaluated models (p-value > 0.30 in all cases). More specifically, the model selected as the most explicative for the average maximums (Mmax) and average minimums (Mmin), were the respective null models (i.e., $M0_{Mmax}$ and $M0_{Mmin}$). These models in both cases yielded higher AIC ($\Delta AIC_{Mmax} = 2.00$; $\Delta AIC_{Mmin} = 1.65$) than the more complex models (i.e., $M4_{Mmax}$ and $M4_{Mmin}$) that included the silvicultural treatment (T) as an additional explicative variable. Although $M4_{Mmax}$ and $M4_{Mmin}$ were the most explicative models in their corresponding batches according to Akaike's Information Criteria ($AIC_{Mmax} = 823.23$; $AIC_{Mmin} = 805.46$), none of the explicative variables (F and T) had a significant effect on these indexes. In addition, $M0_{Mmax}$ and $M0_{Mmin}$ did not significantly differ from the respective most explanatory models according to χ^2 test (p-value > 0.35 in both cases) and the explanatory variable *F. hepatica* (F) significantly affected the index (p-value < 0.05). In consequence, null models were selected as the most explicative (Table 3).

Regarding the minimum value (Vmin) the models containing the diameter (D) as a random factor, yielded lower AIC values but this model did not pass the fitness quality evaluation, being therefore discarded. The variation of Vmin in the models not containing diameter as random factor was explained by the significance of *F. hepatica*. Among these, the most informative was the null model ($M0_{Vmin}$), that only included the presence of *F. hepatica* as explanatory and tree as random variable. This was followed by $M4_{Vmin}$ which also considered the silvicultural treatment. No significant differences were detected between both models according to the χ^2 test (p-value > 0.29), so $M0_{Vmin}$ was selected as the most explicative.

For the maximum variation index (Dmax), the selected model was the null one ($M0_{Dmax}$) since it yielded a lower value of AIC than the next two more complex models $M1_{Dmax}$ and $M2_{Dmax}$ ($\Delta AIC = 2.10$ and $\Delta AIC = 2.15$ respectively; Table 3). The model $M1_{Dmax}$ included the plot as explicative factor while the model $M2_{Dmax}$ included sampling direction aspect as random factor. None of these models significantly differed from one another (p-value = 0.97), therefore, $M0_{Dmax}$ was selected as the most explicative following the parsimony criteria.

Table 3 Selected models (GLMMs) describing the average maximums (Mmax), average minimums (Mmin), minimum value (Vmin), and maximum variation (Mmax-Vmed) regarding the presence of *F. hepatica* (F) and tree (I) as random factor. Random factors are shown in brackets. Df: Degrees of freedom; AIC: Akaike´s Information Criteria; R^2: conditional R^2

Index	Model code	Description	Df	logLik	Deviance	AIC	R^2
Mmax	$M0_{Mmax}$	Mmax ~ F + (I)	1	− 409.66	819.31	825.23	0.66
Mmin	$M0_{Mmin}$	Mmin ~ F + (I)	1	− 400.42	800.85	807.10	0.64
Vmin	$M0_{Vmin}$	Vmin ~ F + (I)	1	− 292.19	584.38	594.09	0.66
Dmax	$M0_{Dmax}$	Dmax ~ F + (I)	1	− 112.78	225.57	240.36	0.46

Table 4 Evaluated generalized linear models to evaluate the presence or absence of *F. hepatica* (F) considering the indices Dmax, Vmin, Mmax and Mmin as explicative variables. Combination of indices into one single variable is shown in square brackets. Selected model in bold

Model code	Description	Df	logLik	Deviance	AIC	ΔAIC
M2p	**F ~ [Dmax x Vmin]**	**1**	**− 89.68**	**179.37**	**183.45**	**0.00**
M1p	F ~ [Dmax + Vmin]	1	− 91.14	182.27	186.36	2.91
M4p	F ~ Dmax + Vmin + Mmin + Mmax	4	− 90.10	180.20	190.63	7.18
M3p	F ~ [Mmax x Mmin]	1	− 95.84	191.69	195.78	12.33

Df: Degrees of freedom; AIC: Akaike´s Information Criteria. x: product

Noteworthy, the null model of the average of energy consumption index (Vmed), which included the presence of *F. hepatica* as explanatory factor, was almost significant (p-value = 0.05).

A total of 20 additional GLMs were computed to determine a useful combination of significant indices to predict the infection by *F. hepatica* (Table 4). The most explicative model (i.e., M2p; Table 4) consisted in a combined index of Dmax multiplied by Vmin and yielded a lower AIC value than the next three more parsimonious models (Table 4). No significant differences were detected between the models M2p and M1p by the χ^2 test (p-value = 1), so M2p was selected. Once the logistic model M2p was computed and the fitness quality was confirmed, the logistic function was derived using model coefficients (Ramsey and Schafer 2013) to provide the equation that estimates probabilities of CRS infection based on experimental values of Dmax and Vmin. This equation was formulated as a new index called "Chestnut Red Stain Danger index" (CRSD; Equation 1; S2; Fig. 2):

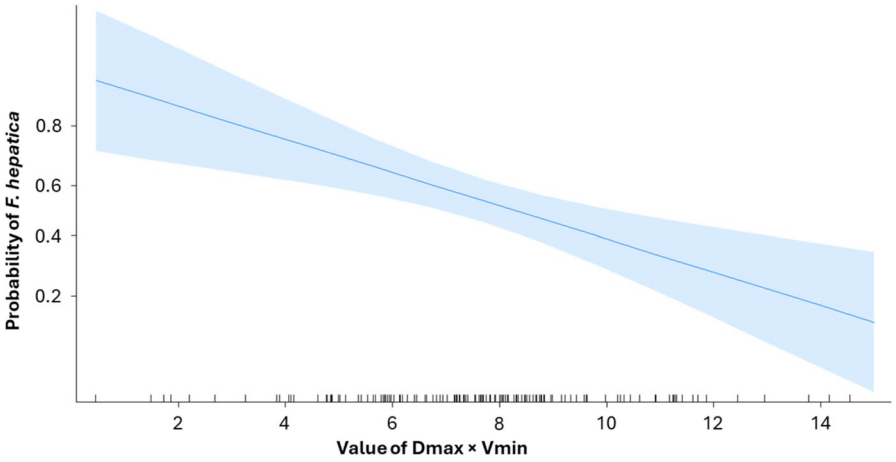

Fig. 2 Probability of infection of *F. hepatica* provided by model M2p. Shaded area: 95% confidence intervals

$$CRSD = \frac{e^{2.248-0.271\cdot(\mathrm{Dmax}\times\mathrm{Vmin})}}{1+e^{2.248-0.271\cdot(\mathrm{Dmax}\times\mathrm{Vmin})}} \quad (1)$$

where CRSD (Chestnut Red Stain Danger index): Estimated probability (0-1) of the presence of *F. hepatica*. Dmax: Maximum variation, index that escalates the difference between the average of maximums (Mmax) with respect to the average of energy consumption (Vmed). Vmin: Minimum value, lowest value of the resistogram that may indicate cracks, cavities, or other anomalies.

Discussion

In this study, the effects of the presence of *F. hepatica*, causal agent of CRS in chestnuts coppices was evaluated through resistance drilling techniques. The results provided here revealed that four of the selected indices (i.e., Mmax, Mmin, Vmin and Dmax) clearly discriminate healthy trees from those infected by *F. hepatica*. Accordingly, the value of these four indices was significantly lower when the trees were infected by the fungus (Table 3).

Our results support the previous studies that show that *F. hepatica* does not produce a significant variation in the overall wood strength at early stages (Vmed, p-value =0.05). Preliminary knowledge of CRS in chestnut wood reports no significant variation of wood density between discolored and normal wood, although some differences were found, such as higher volumetric contraction as well as higher resistance to static bending, lower axial compressive strength and hardness in the CRS-affected wood (Correal-Mòdol 2013). These wood characteristics were assayed on trees presenting only the discoloration and not advanced rot symptoms. So, the results concluded that at those stages CRS had altered some characteristics without jeopardizing the building properties of that wood. This decrease in hardness was also reported on chestnut heartwood presenting color alterations (i.e., reddish heartwood) (Tamantini et al. 2022). Harmful effects on wood strength caused by *F. hepatica* occur only after long periods of colonization, since this fungus can live off the phenolic compounds and tannins of the heartwood cells without damaging the cellulose of the cell walls in early stages (Cartwright 1937; Schwarze, Baum, et al. 2000a, b).

Despite this knowledge that the mechanical properties of the wood are not clearly affected at early stages, we found that *F. hepatica*'s presence in standing trees is detectable through resistance drilling. The average energy consumption to penetration of latewood (Mmax), as happened with the earlywood (Mmin), significantly decreased with the presence of *F. hepatica*. Both indices were reduced by a similar magnitude (i.e., 10.73 and 11.41 %, respectively; Table 3) suggesting that the fungus colonizes early and latewood indistinctively. This idea is supported by the non-detectable effect of *F. hepatica* in the resistance variation index (Vden), consisting of the difference of Mmax and the Mmin (Table 1). This index was developed to detect early rots which often affect earlywood more aggressively (Acuña et al. 2011) and in this case, supports the idea that *F. hepatica* does not specialize in earlywood.

Despite this fungus has not shown a clear preference for early or late wood, the maximum variation index (Dmax) revealed a more detectable effect on the latewood (p-value < 0.05) than on the earlywood (minimum variation index Dmin, p-value > 0.05). Both these indices amplify the disparity of the maximum/minimum mean value concerning the overall mean of energy consumption, emphasizing the differences above or below the overall average in each respective case. Although attacking both types of wood indistinctly, *F. hepatica* causes a more noticeable reduction of the resistance to drilling amplitude on latewood than on earlywood. These results may be due to the importance of the ratio between late and earlywood on the wood's density (Wiedenhoeft 2005) since this ratio varies among species and, in *C. sativa*, latewood is up to three times more abundant than earlywood and contains smaller and fewer vessels, which confers it a higher density (Romagnoli et al. 2011).

The analysis of minimum value (Vmin) suggested that none of the sampled trees exhibited hollowness. In addition, our findings show that the presence of *F. hepatica* significantly decreases the value of this index, as expected for a fungus consuming woody tissues thus indicating that the low-density anomalies would yield lower resistance value after infection takes place. These results agree with the significant reduction of the Mmin index. Even though this index is capable of discriminating the presence or absence of the infection, other anomalies (i.e., cracks or cavities) could also yield very low values. In any case, this would inform of the unsuitability of a particular log for high-quality products and, more importantly, of a particular young tree for producing any high-quality planks after a long rotation.

The evaluated thinning intensities did not significantly affect any of the evaluated resistance drilling indices, suggesting that the methodology developed in this study can be used among these different thinnings indistinctively. The type of thinning was evaluated to determine its effect on wood quality since silvicultural practices can achieve variations of the wood density by modifying stand conditions and number of trees per hectare (Marini et al. 2021; Pretzsch et al. 2018). To analyze the silvicultural effect, variability associated with the plot was controlled by including it as a random factor on several of the models, since site variations have been reported as drivers of wood properties (Romagnoli and Spina 2013).

In this study, a new methodology, based on precise and reliable techniques, was evaluated to detect the presence of the causal agent of CRS in standing trees by testing it against known infected and healthy trees. This methodology provides an accurate and not invasive picture of the health status of the trees since it can detect infections not visible to the naked eye. Our results confirmed the effect of CRS infection in wood properties and supported the utility of four resistance drilling indices (i.e., Mmax, Mmin, Dmax and Vmin) for discriminating trees infected by *F. hepatica* long before harvesting. In addition, the new index CRSD will be a useful tool for forest managers to assess the health status of chestnut coppices at young ages. This methodology will reduce the uncertainty caused by CRS, which is currently the main obstacle to growing high quality chestnut timber in the northeast of Spain. Interestingly, the use of the information provided by the CRSD could be useful beyond productive forest management since *F. hepatica* features in the "Red list of the macrofungi in Poland" under partial protection due to its scarce presence (Piętka and Ciurzycki 2018). Accordingly, the information provided by CRSD could

be helpful for prioritizing forest stands aimed at protection of biodiversity related to old forests.

Conclusion

The presence of *F. hepatica* in *C. sativa* causes a reduction in the wood resistance to drilling that can be detectable at early stages of the rotation by computing common resistance drilling indices (i.e., Mmax, Mmin, Dmax and Vmin). Resistance drilling and the predictive index developed in this work (CRSD) provide an important tool for forest managers to evaluate the health status of chestnut coppices at early ages that can be routinely used in forest management to reduce economic uncertainty. The methodology developed in this work is a new approach to fungal detection and will be useful as a foundation for future research on detection of fungal heart rot infections in standing trees in other forest pathosystems.

Supplementary Information The online version contains supplementary material available at https://doi.org/10.1007/s00226-024-01616-4.

Acknowledgements The study was partially funded by the Diputació de Barcelona. We would like to express our gratitude to Dr. Miriam Piqué and Mr. Mario Beltrán (CTFC) for the use of the study plots they established years ago. Authors also thank Mr. Marcel Vilches for his support and Mr. Amir H. Khalili for his collaboration in the fieldwork.

Authors' contributions AM, EJMA, and CC did the conceptualization. All authors developed the methodology. AM, EJMA, and CC conducted the investigation. AM was responsible for data curation. AM and EJMA performed the formal analysis. AM, EJMA, and CC worked on visualization. AM wrote the original draft. All authors contributed to writing, review, and editing. EJMA and CC provided supervision. ECM and CC supplied resources. CC acquired funding and administered the project.

Funding Open Access funding provided thanks to the CRUE-CSIC agreement with Springer Nature. The study was funded in part by the Diputació de Barcelona.

Data availability Raw data can be found in the CORA public repository: https://doi.org/https://doi.org/10.34810/data1337

Declarations

Conflict of interest The authors declare no competing interests.

Open Access This article is licensed under a Creative Commons Attribution 4.0 International License, which permits use, sharing, adaptation, distribution and reproduction in any medium or format, as long as you give appropriate credit to the original author(s) and the source, provide a link to the Creative Commons licence, and indicate if changes were made. The images or other third party material in this article are included in the article's Creative Commons licence, unless indicated otherwise in a credit line to the material. If material is not included in the article's Creative Commons licence and your intended use is not permitted by statutory regulation or exceeds the permitted use, you will need to obtain permission directly from the copyright holder. To view a copy of this licence, visit http://creativecommons.org/licenses/by/4.0/.

References

Acuña L, Basterra LA, Casado MM, López G, Ramón-Cueto G, Relea E, Martínez C, González A (2011) Aplicación del resistógrafo a la obtención de la densidad y la diferenciación de especies de madera. (Application of resistograph to obtein the density and to differentiate wood species). Materiales de Construcción 61(303):451–464. https://doi.org/10.3989/mc.2010.57610

Barton, K (2020) MuMIn: Multi-Model Inference. R package version 1.43.17. https://CRAN.R-project.org/package=MuMIn

Bates D, Mächler M, Bolker B, Walker S (2015) Fitting Linear Mixed-Effects Models Using lme4. J. Sta. Software. 67(1). https://doi.org/10.18637/jss.v067.i01

Buonincontri MP, Saracino, A, Di Pasquale G (2015) The transition of chestnut (*Castanea sativa* Mill.) from timber to fruit tree: Cultural and economic inferences in the Italian peninsula. The Holocene, 25(7), 1111-1123. https://doi.org/10.1177/0959683615580198

Cartwright KTSG (1937) A reinvestigation into the cause of "brown oak", *Fistulina hepatica* (Huds.) fr. Trans. Br. Mycol. Soc. 21:68–83. https://doi.org/10.1016/S0007-1536(37)80006-6

Conedera M, Tinner W, Krebs P, de Rigo D, Caudullo G (2016) *Castanea sativa* in Europe: Distribution, habitat, usage and threats. In: de Rigo D, Caudullo G, Houston Durrant T, Mauri A (eds) San-Miguel-Ayanz J. European Atlas of Forest Tree Species. publ. Off. EU, Luxembourg, pp 78–79

Conedera M, Manetti MC, Giudici F, Amorini E, (2004) Distribution and economic potential of the Sweet chestnut (*Castanea sativa* Mill.) in Europe. Ecol. Mediterr. 30(2), 179-193. https://doi.org/10.3406/ecmed.2004.1458

Correal-Mòdol E (2013) Propietats químiques, físiques, mecàniques i resistents de la fusta massissa i laminada de castanyer del sistema mediterrani català (Chemical, physical, mechanical and resistance properties of the solid and laminated beech wood from the Catalan Mediterranean system). (Doctoral dissertation). Departament d'Enginyeria Agroforestal, Universitat de Lleida, Lleida, Spain

Dogu D, Kose C, Kartal SN, Erdiz N (2011) Wood identification of wooden marine piles from the ancient Byzantine port of Eleutherius/Theodosius. BioResources 6(2):987–1018

Downes GM, Lausberg M, Potts BM, Pilbeam DL, Bird M, Bradshaw B (2018) Application of the IML Resistograph to the infield assessment of basic density in plantation eucalypts. Australian Forestry 81(3):177–185. https://doi.org/10.1080/00049158.2018.1500676

Fundova I, Funda T, Wu HX (2018) Non-destructive wood density assessment of Scots pine (*Pinus sylvestris* L.) using Resistograph and Pilodyn. PLOS ONE, 13(9), e0204518. https://doi.org/10.1371/journal.pone.0204518

Giovando S, Koch G, Romagnoli M, Paul D, Vinciguerra V, Tamantini S, Marini F, Zikeli F, Scarascia Mugnozza G (2019) Spectro-topochemical investigation of the location of polyphenolic extractives (tannins) in chestnut wood structure and ultrastructure. Ind Crops Prod 141:111767. https://doi.org/10.1016/j.indcrop.2019.111767

Hartig F (2022) DHARMa: Residual Diagnostics for Hierarchical (Multi-Level / Mixed) Regression Models. R package version 0.4.6. http://florianhartig.github.io/DHARMa/

Instrumenta Mechanik Labor System GmbH 2023 Measured Variables of the IML-RESI PowerDrill®Drill Resistance and Feed Force Measurement. *IML – Instrumenta Mechanik Labor System GmbH*

Johnstone D, Ades P, Moore G, Smith I (2007) Predicting wood decay in eucalypts using an expert system and the IML-Resistograph drill. Arboric. Urban For, 33(2), 76-82. https://doi.org/10.48044/jauf.2007.009

Johnstone D, Moore G, Tausz M, Nicolas M (2010) The measurement of wood decay in landscape trees. Arboric. Urban For, 36(3), 121-127. https://doi.org/10.48044/jauf.2010.016

Kappel R, & Mattheck C (2003) Inspection of timber construction by measuring drilling resistance using Resistograph F300-S. 66.

Krebs P, Ulmke F, Tinner W, Conedera M (2022) The roman legacy on European chestnut and walnut arboriculture. Environ. Archaeol., 1-22. https://doi.org/10.1080/14614103.2022.2137648

Marini F, Manetti MC, Corona P, Portoghesi L, Vinciguerra V, Tamantini S, Kuzminsky E, Zikeli F, Romagnoli M (2021) Influence of forest stand characteristics on physical, mechanical properties and chemistry of chestnut wood. Sci. Rep. 11(1):1549. https://doi.org/10.1038/s41598-020-80558-w

Mazerolle MJ (2023) Model selection and multimodel inference based on (Q)AIC(c) (2.3-2) [R]. https://cran.r-project.org/package=AICcmodavg

Meijer A, Muñoz-Adalia EJ, Colinas C (2024) Early thinning: a promising tool to prevent fistulina hepatica heart rot in castanea sativa coppice Stands. Forests 15:1639. https://doi.org/10.3390/f15091639

Oliveira JT, Wang X, Vidaurre GB (2017) Assessing specific gravity of young *Eucalyptus* plantation trees using a resistance drilling technique. Holzforschung 71(2):137–145. https://doi.org/10.1515/hf-2016-0058

Ondrejka V, Gergeľ T, Bucha T, Pástor M (2021) Innovative methods of non-destructive evaluation of log quality. Cent. Eur. For. J. 67(1):3–13. https://doi.org/10.2478/forj-2020-0021

Papandrea SF, Cataldo MF, Zimbalatti G, Proto AR (2022) Comparative evaluation of inspection techniques for decay detection in urban trees. Sens. Actuators, A: Physical, 340, 113544. https://doi.org/10.1016/j.sna.2022.113544

Piętka J, Ciurzycki W (2018) The first record of *Fistulina hepatica* (Schaeff.) With. on *Castanea sativa* Mill. in Poland. Acta Mycol., 53(1). https://doi.org/10.5586/am.1108

Pretzsch H, Biber P, Schütze G, Kemmerer J, Uhl E (2018) Wood density reduced while wood volume growth accelerated in Central European forests since 1870. For. Ecol. Manag. 429:589–616. https://doi.org/10.1016/j.foreco.2018.07.045

R Rcore Team (2023) R Core Team R: A Language and Environment for Statistical Computing; R Foundation for Statistical Computing: Vienna, Austria.

Ramsey FL, Schafer DW (2013) The Statistical Sleuth: A Course in Methods of Data Analysis, 3rd edn. Cengage Learning, Brooks/Cole

Regué A, Bassié L, de-Miguel S, Colinas C (2019) Environmental and stand conditions related to *Fistulina hepatica* heart rot attack on *Castanea sativa*. For. Pathol. 49(3):e12517. https://doi.org/10.1111/efp.12517

Rinn F, Schweingruber FH, Schär E (1996) RESISTOGRAPH and X-Ray Density Charts of Wood. Comparative Evaluation of Drill Resistance Profiles and X-ray Density Charts of Different Wood Species. *Holzforschung*, *50*(4), 303-311. https://doi.org/10.1515/hfsg.1996.50.4.303

Romagnoli M, Cherubini M, Prislan P, Gričar J, Spina S Čufar K (2011) Main Phases of Wood Formation in Chestnut (*Castanea sativa*) in Central Italy—Comparison of Seasons 2008 and 2009. Drvna Ind., 269-275. https://doi.org/10.5552/drind.2011.1124

Romagnoli M, Spina S (2013) Physical and mechanical wood properties of ring-shaken chestnut (*Castanea sativa*) trees. Can. J. For. Res. 43(2):200–207. https://doi.org/10.1139/cjfr-2012-0357

Schwarze FWMR, Baum S, Fink S (2000a) Dual modes of degradation by *Fistulina hepatica* in xylem cell walls of *Quercus robur*. Mycol. Res. 104(7):846–852. https://doi.org/10.1017/S0953756299002063

Schwarze FWMR, Engels J, Mattheck C (2000b) Fungal Strategies of Wood Decay in Trees. Springer, Berlin

Tamantini S, Bergamasco S, Portoghesi L, Vettraino AM, Zikeli F, Mugnozza GS, Romagnoli M (2022) Detection, description, and technological properties of colour aberration in wood of standards and shoots from a chestnut (*Castanea sativa* Mill.) coppice stand. Eur. J. For. Res., 141(4), 683-698. https://doi.org/10.1007/s10342-022-01468-2

Thaler N, Žlahtič M, Humar M (2014) Performance of recent and old sweet chestnut (*Castanea sativa*) wood. Int. Biodeter. Biodegr. 94:141–145. https://doi.org/10.1016/j.ibiod.2014.06.016

Vericat P, Navarro P, Correal-Mòdol E, Castaño C, Piqué M, Beltrán M, Óbón B, Rodriguez J, Colinas C, García M, Argemí J, Rovira J (2012) *El castanyer a Catalunya: Manual de gestió, conservació i valorització* (The chestnut tree in Catalonia: Manual of management, conservation and valorisation). (Diputació de Barcelona i Obra Social "la Caixa").

Wang X & Allison RB (2008) Decay Detection in Red Oak Trees Using a Combination of Visual Inspection, Acoustic Testing, and Resistance Microdrilling. Arboriculture & Urban Forestry, 34(1), 1-4. https://doi.org/10.48044/jauf.2008.001

Wiedenhoeft A (2005) Structure and Function of Wood. In *Handbook of Wood Chemistry and Wood Composites* (pp. 9-33). Taylor & Francis Group.

Yurkewich JI, Castaño C, Colinas C (2017) Chestnut Red Stain: Identification of the fungi associated with the costly discolouration of *Castanea sativa*. For. Pathol. 47(4):e12335. https://doi.org/10.1111/efp.12335

Publisher's Note Springer Nature remains neutral with regard to jurisdictional claims in published maps and institutional affiliations.